

## **Bidirectional single sideband transmission of Millimeter Waves over Fiber for 5G Mobile Networks**

### **Transmisión bidireccional en banda lateral única de ondas milimétricas sobre fibra para redes móviles 5G**

Alejandro Patiño-Carrillo<sup>1</sup>, Gustavo Puerto-Leguizamón<sup>2</sup>,  
y Carlos Suárez-Fajardo<sup>3</sup>

Recibido: 04 de junio de 2018  
Aceptado: 03 de septiembre de 2018

---

#### Cómo citar / How to cite

A. Patiño-Carrillo, G. Puerto-Leguizamón, y C. Suárez-Fajardo, Bidirectional single side band transmission of Millimeter Waves over Fiber for 5G Mobile Networks. *TecnoLógicas*, vol. 21, no. 43, pp. 15-26, 2018.

© Instituto Tecnológico  
Metropolitano

Este trabajo está licenciado bajo una  
Licencia Internacional Creative  
Commons CC BY-NC-SA



---

<sup>1</sup> MSc in Mobile Communications, Faculty of Engineering, Universidad Distrital Francisco José de Caldas, Bogotá-Colombia, apatinoc@correo.udistrital.edu.co

<sup>2</sup> PhD in Telecommunications, Faculty of Engineering, Universidad Distrital Francisco José de Caldas, Bogotá-Colombia, gapuerto@udistrital.edu.co

<sup>3</sup> PhD in Telecommunications, Faculty of Engineering, Universidad Distrital Francisco José de Caldas, Bogotá-Colombia, csuarezf@udistrital.edu.co

### **Abstract**

This study proposes, experimentally demonstrates, and simulates a network architecture for the transport of millimeter waves (MMW) based on Radio over Fiber (RoF) techniques for the transport of signals in the fronthaul segment of the next 5G generation mobile systems. Such approach exploits the benefits of bidirectional single-sideband modulation in order to generate an optical subcarrier for the downlink transmission and a second subcarrier for the transport of the uplink services, as well as the centralization of optical sources. The proposed architecture is evaluated based on the analyses of the Bit Error Rate (BER) performance and Error Vector Magnitude (EVM) in both downlink and uplink. Likewise, simulation modeling of the approach was conducted in order to evaluate the quality of the MMW signals at different frequencies available in the MMW spectrum. The results show a power penalty lower than 2 dB for a  $1 \times 10^{-12}$  BER and an EVM below 12% within a power margin of 6 dB, which demonstrates the feasibility of the approach.

### **Keywords**

Millimeter Waves, Radio Over Fiber, 5G-fifth generation mobile, Optical centralization

### **Resumen**

Una arquitectura de red para el transporte de ondas milimétricas (MMW) basada en las técnicas de Radio sobre Fibra (RoF) para el transporte de señales en el segmento de fronthaul de los futuros sistemas 5G se propone, se demuestra experimentalmente y se simula en este artículo. La propuesta aprovecha los beneficios de una doble modulación en banda lateral única para generar una subportadora óptica para la transmisión en el enlace descendente y una segunda subportadora para el transporte de los servicios en el enlace ascendente, así como la centralización de las fuentes ópticas. La evaluación de la arquitectura propuesta se basa en el análisis del rendimiento de la Tasa de Error de Bit (BER) y la Magnitud de Vector de Error (EVM) tanto en el enlace descendente como en el enlace ascendente. Del mismo modo, se realizó un modelo de simulación de la propuesta para evaluar la calidad de las señales en MMW a diferentes frecuencias del espectro disponible de MMW. Los resultados muestran una penalización en potencia de 2 dB para un BER de  $1 \times 10^{-12}$  y un EVM inferior al 12% en un margen de potencia de 6 dB, demostrando la factibilidad del sistema propuesto.

### **Palabras clave**

Ondas Milimétricas, Radio Sobre Fibra, 5G-quinta generación móvil, centralización óptica.

## 1. INTRODUCTION

According to the Cisco Visual Networking Index (VNI) Report on Global Mobile Data Traffic 2016-2021, by 2021, there will be around 5,500 million mobile phones in the world. The exponential increase in mobile users, smartphones, broadband Internet connections, the Internet of Things paradigm, and the growing consumption of mobile video will multiply fixed and mobile data traffic sevenfold over the next four years [1].

This is one of the reasons why cellular mobile networks continue their evolution from previous generations towards 5G, whose project (IMT-2020 and Beyond) developed by ITU-3GPP, started in 2012 with a time horizon of eight years [2]. Among the innovations this next generation will bring is the use of a new frequency spectrum called millimeter waves (MMW), whose range lies between 30 and 300 GHz [3]. This spectrum will mitigate current limitations imposed by the saturation of frequencies up to 5 GHz. The use of frequencies in the millimeter band is considered one of the cornerstones that will support the fronthaul segment in future 5G networks [4]. In this context, transmission techniques based on Radio over Fiber (RoF) emerged as a mechanism that allows the convergent transport and distribution of high frequency signals [5]. Said convergent process, in addition, has the great advantage of being able to use the current infrastructure of wireless networks, thus reducing costs and deployment times. This characteristic addresses the previously mentioned access needs and it offers alternatives for the provision of services (such as triple play), trends in cloud computing [6], Distributed Antenna Systems (DAS) [7] and, in general, an environment with a growing number of users. These subscribers demand quality in telecommunications services, and they essentially use fiber optics as transmission lines and radio

systems to enable wireless access and mobility.

On the other hand, RoF transmission techniques facilitate the centralization of Baseband Units (BBU) because the complex signal processing in the central office (CO) and the base station (BS) is very simple, passive, and compact, which results in less restrictive operation and maintenance. This kind of systems can easily serve densely populated areas with high peaks of traffic and support multiple wireless standards to increase bandwidth. These capacities enable to reduce processing times and improve operations in dense or small-cell wireless networks given the nature of the propagation of MMW signals in free space [8]. By reducing the cell size, limited spectral resources can be reused between small cells more frequently, thus increasing the total capacity of the system. The combination of small-cell architecture and higher RF bands offers a promising solution to dramatically increase the capacity of mobile systems by using the new frequency band [9], [10].

Previous works on optical transport for 5G systems have reported the transmission of 60 GHz over a 25-km downlink employing the optical heterodyning of a laser [11]. For instance, a downlink RoF technique that can support the distribution of broadband wireless signals in a converged optical/wireless system using digitized radio signals and optical single sideband is presented in [12]. An architecture for high-speed multi-service data transmission based on the concept of centralized BBU is detailed in [13]. Also, the exploitation of an optical single sideband and dual sideband carrier suppressed in the downlink of the fronthaul segment is described and analyzed in [14]. Moreover, a bidirectional mobile fronthaul system based on Wavelength Division Multiplexing (WDM) and non-MMW digitized Frequency Division Multiplexing (FDM) applied to

support independent asynchronous small cells is outlined in [15]. Finally, a bidirectional RoF system for small cells that uses high speed electro-optical converters in both directions is introduced in [16].

This study proposes, experimentally demonstrates, and simulates an architecture for bidirectional transmission of millimeter-band carriers featuring BBU centralization. Such proposal is based on the transmission of a bidirectional optical single-sideband subcarrier generated by a Mach-Zehnder electro-optical modulator [17]. One of the single-sideband subcarriers enables the downlink; another subcarrier, the uplink. This system also allows to centralize the optical source by preventing the use of optical sources on the base station side.

Fig. 1 shows the environment for the proposed architecture, in which the BBUs are centralized in the CO and the millimeter-band carriers are transported as optical subcarriers in the Optical Distribution Network (ODN) [18], between the CO and BS and vice versa.

This work is organized as follows: Section 2 presents the mathematic foundations of optical single-sideband modulation and the description of the proposed architecture. Section 3 describes the experimental results and, finally, section 4 summarizes the study.

## 2. MATERIALS AND METHODS

### 2.1 Theoretical description

The electric field at the output of the optical modulator is defined, based on the modulator geometry, as a function of the incoming electric field and the phase shifts induced by the electrical signals applied to the electrodes of the MZ modulator as a consequence of the electro-optical effect. When an electrical signal is applied to one of the two arms of the interferometer, it causes a phase change in the propagated optical signal due to the electro-optical effect.

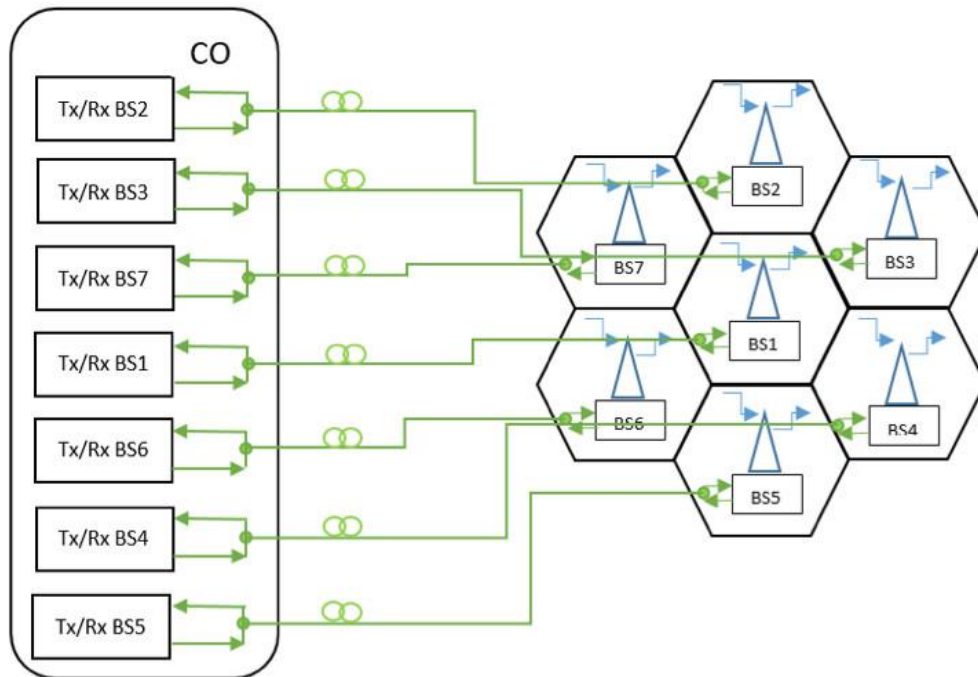


Fig. 1. Centralization of BBUs for small cells in a 5G environment. Source: Authors' own work.

The general expression of the electric field at the output of the MZM modulator is given by (1):

$$E_{out}(t) = \left(\frac{1}{4}\right) E_{in}(t) [\exp(j\Delta\phi_1) + \exp(\pm j\Delta\phi_2)] \quad (1)$$

In turn, the terms of the phase variation  $\phi_n$  depend on the bias voltage  $V\pi$ . Such value is defined as the voltage applied to the electrodes of the device that causes a phase change of  $180^\circ$  in the optical signal that propagates in the waveguide. Likewise,  $V_{RF}$  represents the voltage amplitude in the RF inputs (upper and lower). Therefore, the phase variation as a function of these voltages can be expressed by (2) and (3):

$$\Delta\phi_1 = \frac{\pi}{V_{\pi(RF)}} V_{1(RF)}(t) + \frac{\pi}{V_{\pi(dc)}} V_{1(dc)} \quad (2)$$

$$\Delta\phi_2 = \frac{\pi}{V_{\pi(RF)}} V_{2(RF)}(t) + \frac{\pi}{V_{\pi(dc)}} V_{2(dc)} \quad (3)$$

It is worth mentioning that, since the optical carrier does not convey information, terms  $V_1$  (dc) and  $V_2$  (dc) are null in our proposal. In order to obtain a single-sideband RoF system, two RF frequencies

are electrically combined and shifted  $90^\circ$  with respect to each other before being applied to the two arms of the optical modulator. The two copies of the  $90^\circ$  phase-shifted RF signals are expressed by (4) and (5):

$$em_1(t) = e(t) \cos(\omega_e t + \alpha_e) \quad (4)$$

$$em_2(t) = e(t) \sin(\omega_e t + \alpha_e) \quad (5)$$

where  $e(t)$  represents the information band;  $\omega_e t$ , the subcarrier's frequency; and  $\alpha_e$ , the phase signal. Therefore, the expressions that define the electrical signals at the input of the modulator are given by (6) and (7).

Equations (1), (2), (3), (6), and (7) were used to obtain the general equation that defines the electrical field at the output of the modulator for a single-sideband optical modulation (8).

Note that the exponential and cosine of the argument are zero for one of the two expressions ( $em_1$  or  $em_2$ ) when there is a  $90^\circ$  phase shift between them, thus a single-sideband modulated signal is obtained. The expression for the optical output power is based on (8) and given by (9).

$$V_{1(RF)}(t) = \frac{1}{2} + \frac{1}{\sqrt{2}} e(t) \cdot \cos(\omega_e t + \alpha_e) \quad (6)$$

$$V_{1(RF)}(t) = \frac{1}{2} + \frac{1}{\sqrt{2}} em_1(t)$$

$$V_{2(RF)}(t) = \frac{1}{2} + \frac{1}{\sqrt{2}} e(t) \cdot \cos(\omega_e t + \alpha_e - \pi/2)$$

$$V_{2(RF)}(t) = \frac{1}{2} + \frac{1}{\sqrt{2}} e(t) \cdot \sin(\omega_e t + \alpha_e) \quad (7)$$

$$V_{2(RF)}(t) = \frac{1}{2} + \frac{1}{\sqrt{2}} em_2(t)$$

$$E_{out}(t) = \frac{1}{2} E_{in}(t) \exp\left\{j\frac{\rho}{2\sqrt{2}V_{\rho(RF)}}(em_1(t) - em_2(t))\right\} + \frac{1}{2} \exp\left\{j\frac{\rho}{2\sqrt{2}V_{\rho(RF)}}(em_1(t) + em_2(t))\right\} \quad (8)$$

$$P_{out}(t) = \frac{P_{in}}{8} \left[ 1 + \sin\left(\frac{\rho}{V_{\rho(RF)}}\right) \cos\left(\frac{\rho}{\sqrt{2}V_{\rho(RF)}}(em_1(t) + em_2(t))\right) + \cos\left(\frac{\rho}{V_{\rho(RF)}}\right) \sin\left(\frac{\rho}{\sqrt{2}V_{\rho(RF)}}(em_1(t) + em_2(t))\right) \right] \quad (9)$$

## 2.2 Architecture description

Fig. 2 outlines a bidirectional single-sideband millimeter-wave network over fiber for the fronthaul link of future 5G networks. The layout of the downlink is illustrated on top and the uplink, at the bottom. This system allows the centralization of optical sources through the simultaneous conformation of two single-sideband optical modulation schemes. In the CO, a double control MZM powered by a laser diode is used at a frequency of 1532.7 nm and an optical power of 0dBm. Two types of services were transmitted by two different subcarriers over the downlink. The first service consisted of a 1-Gb/s baseband signal encoded in NRZ over 6 GHz; the second was a signal at 10 MBauds, 16QAM modulated onto 6 GHz. One of these services was injected by one of the arms of the optical modulator. On the other arm, a subcarrier was injected at 13 GHz without modulation (this tone will be used as a carrier for the uplink). The two RF subcarriers were shifted 90° by a hybrid coupler before feeding each one of the arms of the optical modulator. With this configuration, one of the sidebands of each

subcarrier is eliminated and a spectral response is obtained at the output (Fig. 2, inset a). This combination of signals is sent through a single-mode fiber span of 5 km with optical amplification using an Erbium-Doped Fiber Amplifier (EDFA) with a gain of 20 dB. At the base stations (BS), the proposed design consists of a Fiber Bragg Grating (FBG) centered at the optical frequency of the 6-GHz modulated signal. This subcarrier is filtered and dropped by a circulator, thus allowing other spectral components to pass through. The signal reflected in 6 GHz is received by a PIN photodetector and filtered by a band pass filter (BPF) to obtain the subcarrier that will be radiated from the BS to the users. The optical signal transmitted through FBG contains the 13-GHz unmodulated RF signal on which the uplink information will be transported (Fig. 2, inset b). Similarly, two types of services were transmitted in the uplink: (1) a baseband signal at 1 Gb/s encoded in NRZ and (2) a signal at 10 MBauds, QPSK modulated at 13 GHz. After fiber transmission, the uplink signal is received and processed in the CO in order to evaluate its quality.

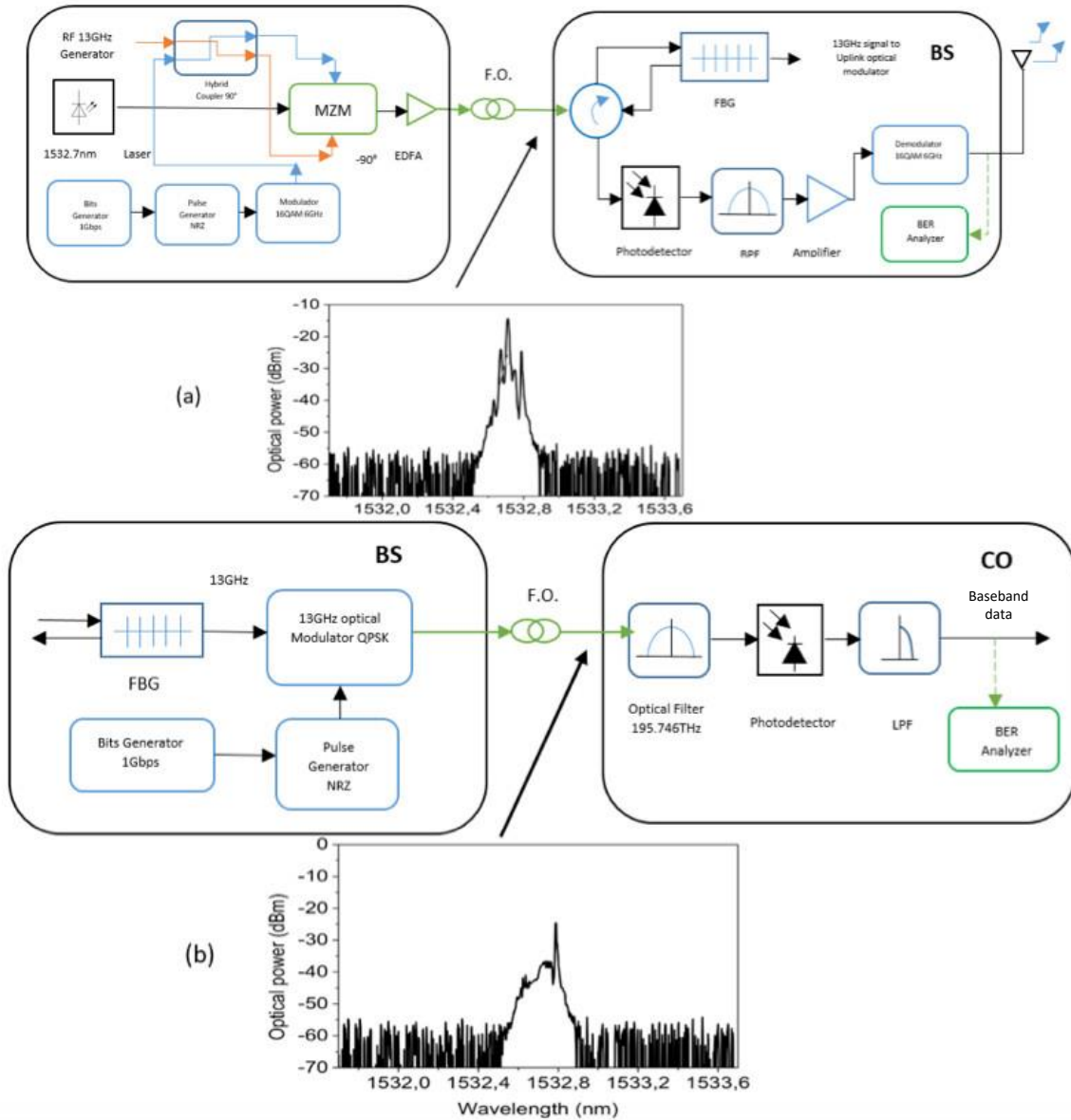


Fig. 2. Layout of the bidirectional single-sideband approach for the transport of MMW. Top: Downlink. Bottom: Uplink. Inset (a): Optical spectrum at the input of the BS. Inset (b): Optical spectrum at the input of the CO. Source: Authors' own work.

### 2.3 Simulation modeling

The proposed approach was evaluated by assessing the signal quality of the transported services according to the millimeter wave and bit rate that were used. To this aim, a layout featuring the architecture shown in Fig 2(a) was implemented in Optisystem v14. Said layout consisted of a binary generator with a bit rate of 1 Gb/s, an NRZ pulse encoder,

and an amplitude modulator, whose operating frequency was swept from 12 to 60 GHz in increments of 6 GHz and fed to one port of a dual-arm Mach-Zehnder optical modulator. The other arm was fed a modulated 10-GHz subcarrier conveying a 1-Gb/s bit rate. In addition, a laser with a frequency of 193.1 THz was used. The RoF transmitter fed a 10-km standard single-mode coil of fiber featuring an attenuation constant of 0.2 dB/km and a dispersion

parameter of 16.75 ps/km.nm. A carrier suppression filter with a bandwidth of 5 GHz was introduced on the receiver’s side. The purpose of said filter is to eliminate the optical carrier and only allow the sidebands in order to mitigate the carrier suppression effect. After photo-detection, the central frequency of a 10-GHz pass-band filter was swept following the same configuration of the transmitter in order to estimate the quality of the transported signals.

### 3. RESULTS

Experimental evaluations measured the signal quality of services transmitted from the CO and BS in both the downlink and the uplink. Fig. 3 presents the assessment of the Bit Error Rate (BER) performance of the 1-Gb/s service under study onto 6 GHz (RF-1) and also onto 8 GHz (RF-2). It shows a penalty of approximately 2.3 dB and 1.8 dB, respectively, for  $1 \times 10^{-12}$  BER compared to the back-to-back curves. Fig. 4 shows the quality of the 16QAM service onto 6 GHz (RF-1) and 8 GHz (RF-2).

Signal degradation was measured and an Error Vector Magnitude (EVM) below 11% was found for optical powers received above -25 dBm, which exhibited a degradation of approximately 7% compared to the back-to-back value. Besides the penalty due to the inherent insertion losses of the optical devices and fiber propagation, the nonlinear response of the optical modulator imposes a sideband suppression in the order of 20 dB. Thus, the harmonics of both subcarriers derive in crosstalk between them. This fact affects the baseband service to a greater extent due to the higher number of frequency components compared to the digital 16QAM service.

The results show that an EVM power margin of 6 dB is feasible (measurements were performed between -25 dBm and -31 dBm, as can be seen in Fig. 4). The power margin is defined as the difference between the maximum and minimum received RF power that satisfies the EVM limit value. In particular, the EVM limit for the 3rd Generation Partnership Project (3GPP), the Universal Mobile Telecommunications System (UMTS), and Long Term Evolution (LTE) using 16QAM modulation is 12.5% [19].

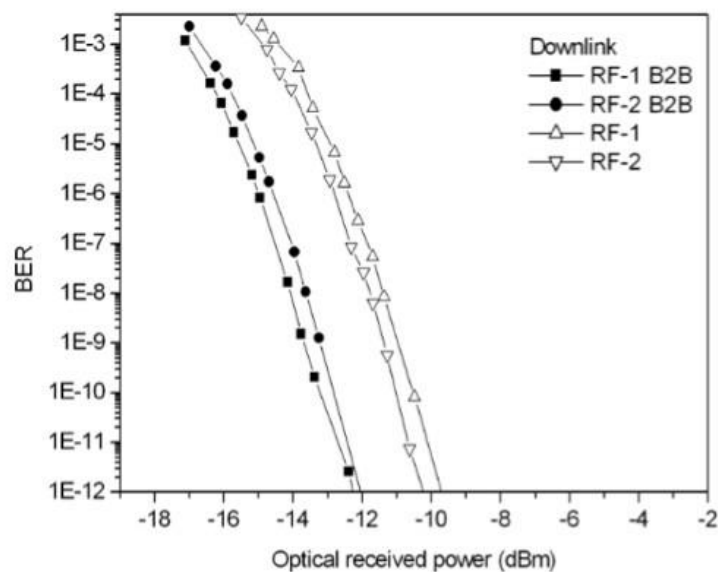


Fig. 3. Experimental results: Downlink BER. Source: Authors’ own work.

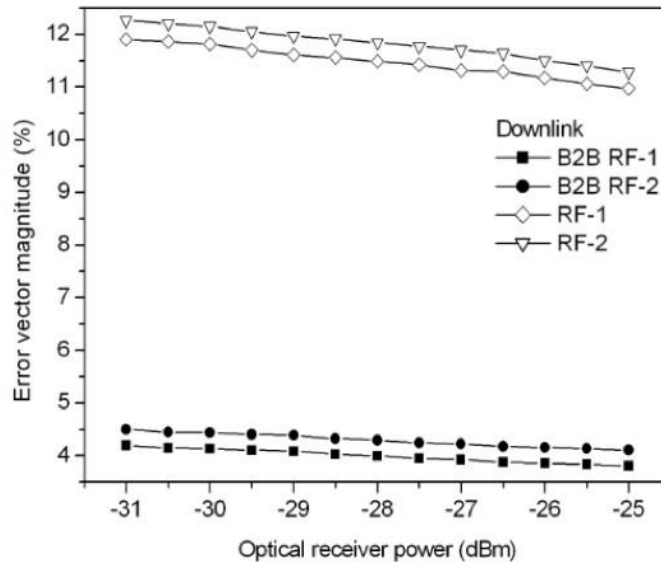


Fig. 4. Experimental results: Downlink EVM. Source: Authors' own work.

The experimental results of the quality of the baseband uplink signals are shown in Fig. 5. Overall, the full penalty was measured at 0.9 dB for  $1 \times 10^{-12}$  BER of the 1-Gb/s service onto 13 GHz (RF-1), and at 1.6 dB onto 15 GHz (RF-2). Fig. 6 shows the results obtained from the QPSK service. The measured EVM is approximately 6.3% for received powers below -25 dBm, with an average degradation of 2.3% compared to the back-to-back of the signal onto 13 GHz (RF-1). Also, such EVM reaches 6.5% for received powers below -25 dBm, with a degradation of 2.1% onto 15 GHz (RF-2).

As can be noticed, the degradation of the uplink signals is caused by the crosstalk after the filtering process in the FBG, which results in remaining signals in the process of detection and down conversion. Nevertheless, it can also be observed that the results of the uplink signal are less penalized than those of its downlink counterpart. The uplink signals also satisfy the EVM limit, since acceptable values for QPSK services should reach a maximum EVM value of 17.5% [19].

Finally, in order to characterize the quality of the obtained signal as a function

of the frequency in millimeter band and transmitted bit rate, the system was modeled using OptiSystem. This simulation software assessed the behavior of the proposed architecture between 12 GHz up to 84 GHz for transmission rates of 1 Gb/s, 2 Gb/s, and 5 Gb/s. As can be seen in Fig. 7, the quality factor of the signal decreases as a function of the transmission rate, but it remains constant as a function of the employed millimeter region. The significant penalties for transmission rates higher than 1 Gb/s are due to a higher level of intermodulation caused by the Composite Second Order (CSO) distortion introduced by the non-linear response of the modulator.

Finally, a comparison between our approach and similar proposals (such as those described in [15] and [16]), reveals a noticeable difference: in this study, optical sources are centralized by means of single-sideband optical modulation. This feature is enabled by shifting  $90^\circ$  the phase of the electrical subcarriers at the input of the optical modulator. Such process requires a linear response of both the microwave shifters and the optical modulator in order to reduce the effects described in the previous paragraph.

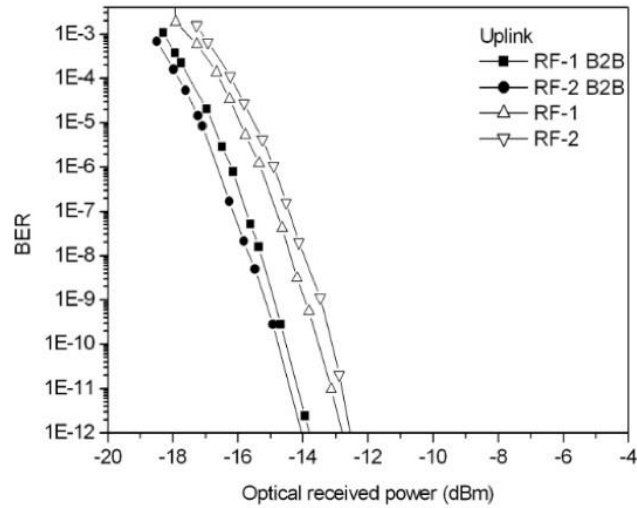


Fig. 5. Experimental results: Uplink BER. Source: Authors' own work.

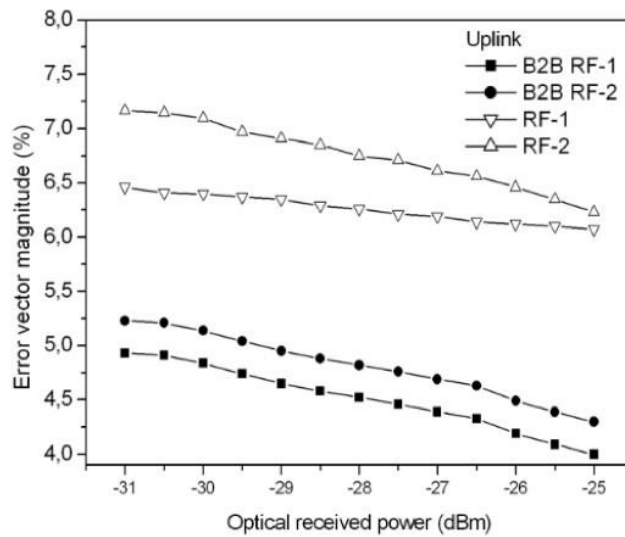


Fig. 6. Experimental results: Uplink EVM. Source: Authors' own work.

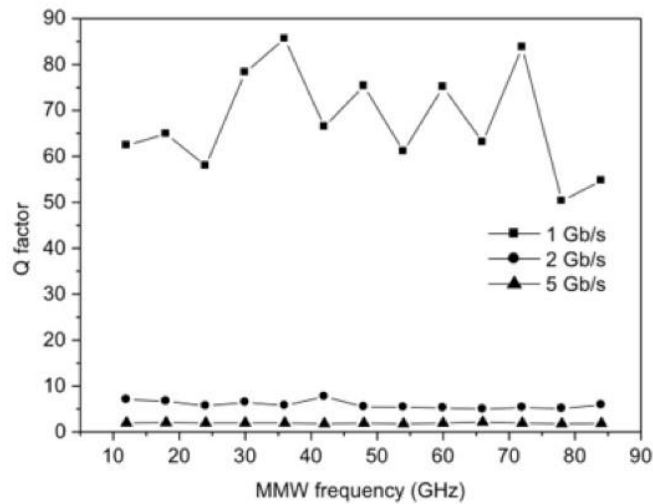


Fig. 7. Simulation results: Q factor as a function of the MMW frequency. Source: Authors' own work.

#### 4. CONCLUSIONS

This paper demonstrated a millimeter wave radio-over-fiber network architecture that allows bidirectional transmission of signals in the context of a future 5G mobile environment. The novelty of our approach is the centralization of both mobile baseband units and optical sources by simultaneously building two single-sideband optical modulation schemes. One of the subcarriers conveys the downlink information and the other subcarriers in the base station transport the uplink. A mathematical description of the single-sideband optical modulation process was also presented.

As far as the experimental demonstration is concerned, the Bit Error Rate (BER) performance of the 1-Gb/s service onto 6 GHz (RF-1) and 8 GHz (RF-2) showed penalties of approximately 2.3dB and 1.8dB, respectively, compared to the back-to-back curves. The EVM of the 16QAM service onto the same carriers was below 11% at -25dBm and 7% compared to back-to-back degradation. These measurements are satisfactory compared to the 3GPP standard, which indicates it should be lower than 12.5% for 16QAM digital modulation.

The penalties of the uplink for the 1-Gb/s baseband service and a BER of  $1 \times 10^{-12}$  were 0.9 dB for the 13-GHz carrier and 1.6 dB for the 15-GHz carrier. For the QPSK service, the EVM obtained at -25dBm onto 13 GHz was 6.3% and onto 15 GHz, 6.5%. They suffered a degradation of 2.3% and 2.1%, respectively, compared to back-to-back curves. These values are even more satisfactory in terms of the 3GPP standard, which establishes they should be lower than 17.5% for QPSK modulation.

When the response of the quality factor (Q) was characterized as a function of the frequency and the bit rate, a remarkable degradation of the Q was observed in rates higher than 1 Gb/s. These results show that the approach performs well regardless

of the MMW employed, but the distortions increase proportionally to the bit rate. The process to generate the RoF signal of two subcarriers using only one modulator causes a great numerical difference in terms of quality at different bit rates, because the intermodulation distortion spreads all over the spectrum. In the context of a future 5G mobile network, careful attention must be paid to the setup of the Mach-Zehnder modulator, since the bandwidth and extinction ratio must guarantee that the modulation indexes of both single-sideband subcarriers does not surpass its dynamic range. In addition, alternative approaches such as the use of two independent modulators should also be evaluated in order to ensure the capacity to transport higher bit rates.

#### 5. ACKNOWLEDGMENTS

The authors wish to acknowledge and thank *Universidad Distrital Francisco José de Caldas* and *ITEAM Research Institute* for supporting the development of this study.

#### 6. REFERENCES

- [1] Cisco, "Cisco Visual Networking Index: Global Mobile Data Traffic Forecast Update, 2016–2021 White Paper," *Cisco public*, 2017. [Online]. Available: <https://www.cisco.com/c/en/us/solutions/collateral/service-provider/visual-networking-index-vni/mobile-white-paper-c11-520862.html>.
- [2] J. G. Andrews *et al.*, "What Will 5G Be?," *IEEE J. Sel. Areas Commun.*, vol. 32, no. 6, pp. 1065–1082, Jun. 2014.
- [3] S. Rangan, T. S. Rappaport, and E. Erkip, "Millimeter-Wave Cellular Wireless Networks: Potentials and Challenges," *Proc. IEEE*, vol. 102, no. 3, pp. 366–385, Mar. 2014.
- [4] T. S. Rappaport, Y. Xing, G. R. MacCartney, A. F. Molisch, E. Mellios, and J. Zhang, "Overview of Millimeter Wave Communications for Fifth-Generation (5G)

- Wireless Networks—With a Focus on Propagation Models,” *IEEE Trans. Antennas Propag.*, vol. 65, no. 12, pp. 6213–6230, Dec. 2017.
- [5] Jianping Yao, “Microwave Photonics,” *J. Light. Technol.*, vol. 27, no. 3, pp. 314–335, 2009.
- [6] M. Maier and B. P. Rimal, “Invited paper: The audacity of fiber-wireless (FiWi) networks: revisited for clouds and cloudlets,” *China Commun.*, vol. 12, no. 8, pp. 33–45, Aug. 2015.
- [7] P. Chanclou *et al.*, “How Does Passive Optical Network Tackle Radio Access Network Evolution?,” *J. Opt. Commun. Netw.*, vol. 9, no. 11, p. 1030, Nov. 2017.
- [8] R. Abdolee, R. Ngah, V. Vakilian, and T. A. Rahman, “Application of radio-over-fiber (ROF) in mobile communication,” in *2007 Asia-Pacific Conference on Applied Electromagnetics*, 2007, pp. 1–5.
- [9] Gee-Kung Chang, Lin Cheng, Mu Xu, and D. Guidotti, “Integrated fiber-wireless access architecture for mobile backhaul and fronthaul in 5G wireless data networks,” in *2014 IEEE Avionics, Fiber-Optics and Photonics Technology Conference (AVFOP)*, 2014, vol. 4, pp. 49–50.
- [10] M. Agiwal, A. Roy, and N. Saxena, “Next Generation 5G Wireless Networks: A Comprehensive Survey,” *IEEE Commun. Surv. Tutorials*, vol. 18, no. 3, pp. 1617–1655, 2016.
- [11] C. Browning, E. P. Martin, A. Farhang, and L. P. Barry, “60 GHz 5G Radio-Over-Fiber Using UF-OFDM With Optical Heterodyning,” *IEEE Photonics Technol. Lett.*, vol. 29, no. 23, pp. 2059–2062, Dec. 2017.
- [12] D. Novak *et al.*, “Radio Over Fiber Technologies for Emerging Wireless Systems,” *IEEE J. Quantum Electron.*, vol. 52, no. 1, pp. 1–11, Jan. 2016.
- [13] C. Liu, J. Wang, L. Cheng, M. Zhu, and G.-K. Chang, “Key Microwave-Photonics Technologies for Next-Generation Cloud-Based Radio Access Networks,” *J. Light. Technol.*, vol. 32, no. 20, pp. 3452–3460, Oct. 2014.
- [14] Y. Tian, K. L. Lee, C. Lim, and A. Nirmalathas, “60 GHz Analog Radio-Over-Fiber Fronthaul Investigations,” *J. Light. Technol.*, vol. 35, no. 19, pp. 4304–4310, 2017.
- [15] M. Xu *et al.*, “Bidirectional Fiber-Wireless Access Technology for 5G Mobile Spectral Aggregation and Cell Densification,” *J. Opt. Commun. Netw.*, vol. 8, no. 12, p. B104, Dec. 2016.
- [16] P. T. Dat, A. Kanno, and T. Kawanishi, “Radio on radio over fiber: efficient fronthauling for small cells and moving cells,” *IEEE Wirel. Commun.*, vol. 22, no. 5, pp. 67–75, Oct. 2015.
- [17] K. P. Ho and H. W. Cui, “Generation of arbitrary quadrature signals using one dual-drive modulator,” *J. Light. Technol.*, vol. 23, no. 2, pp. 764–770, 2005.
- [18] M. Cely, R. Muñoz, G. Puerto, and C. Suárez, “Generación de señales para sistemas de radio sobre fibra basados en la combinación eléctrica de componentes de banda base y radiofrecuencia,” *Ingeniare. Rev. Chil. Ing.*, vol. 24, no. 3, pp. 403–411, Jul. 2016.
- [19] Rohde & Schwarz, O. Werther, and R. Minihold, “LTE System Specifications and their Impact on RF & Base Band Circuits,” 2013.